Supplementary Information (SI) for Journal of Materials Chemistry C.

Supporting Information

Design of moderate-pressure superconductivity in the ternary hydride system

Contents

Xue Li[a*], Nan Wang[a], Yuan Ma[c], JingKai Bi[b], Hanyu Liu[c*]

a. Henan Institute of Advanced Technology, Zhengzhou University, Zhengzhou 450001, China
b. Institute of Quantum Materials and Physics, Henan Academy of Sciences, Zhengzhou 450001, China
c. Key Laboratory of Material Simulation Methods and Software of Ministry of Education, College of Physics, Jilin University, Changchun 130012, China

Contents

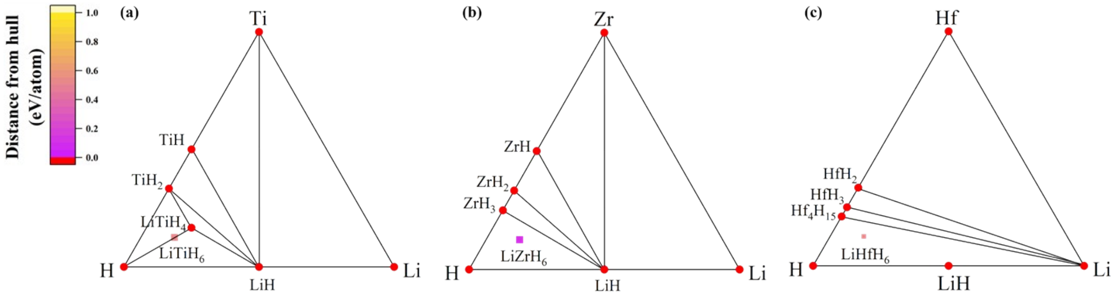

Figure S1. The convex hulls for $LiTiH_6$, $LiZrH_6$, and $LiHfH_6$ at 50 GPa.

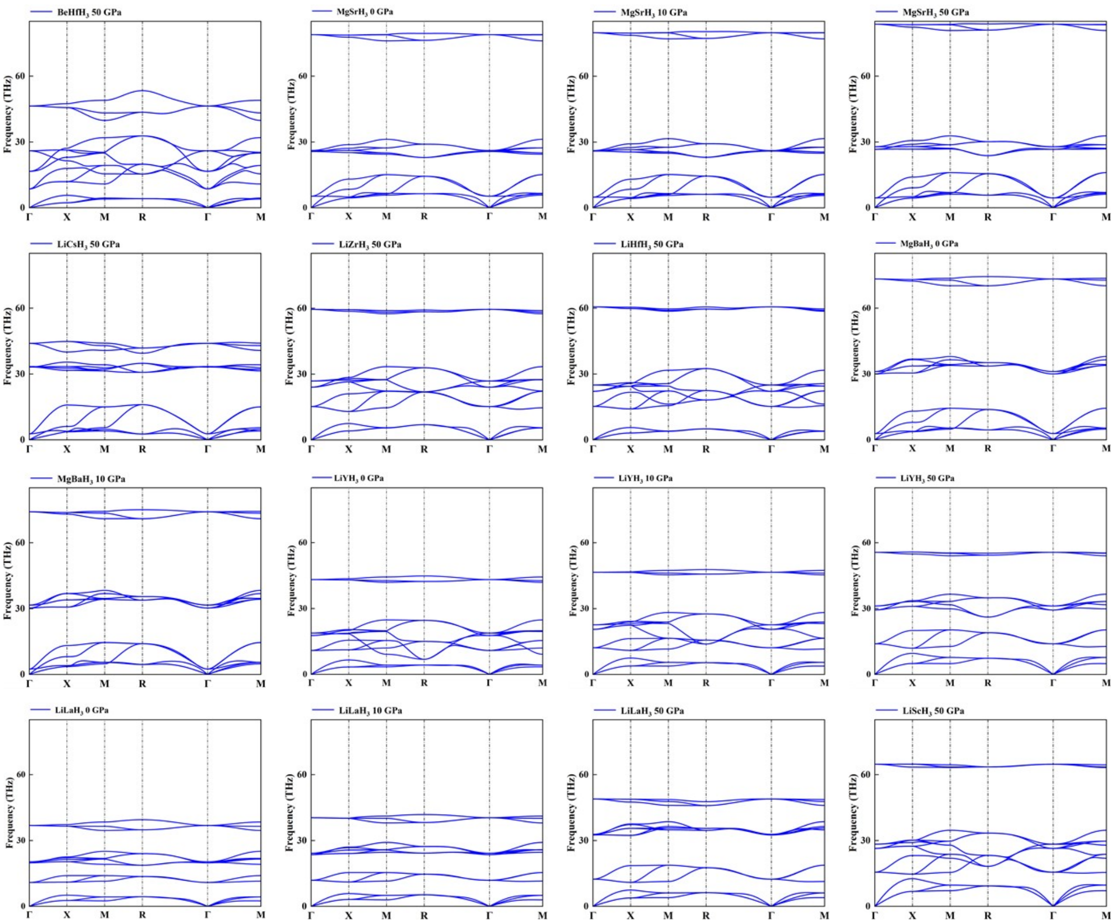

Figure S2. Calculated phonon spectrum of newly predicted ABH_3 under different pressure.

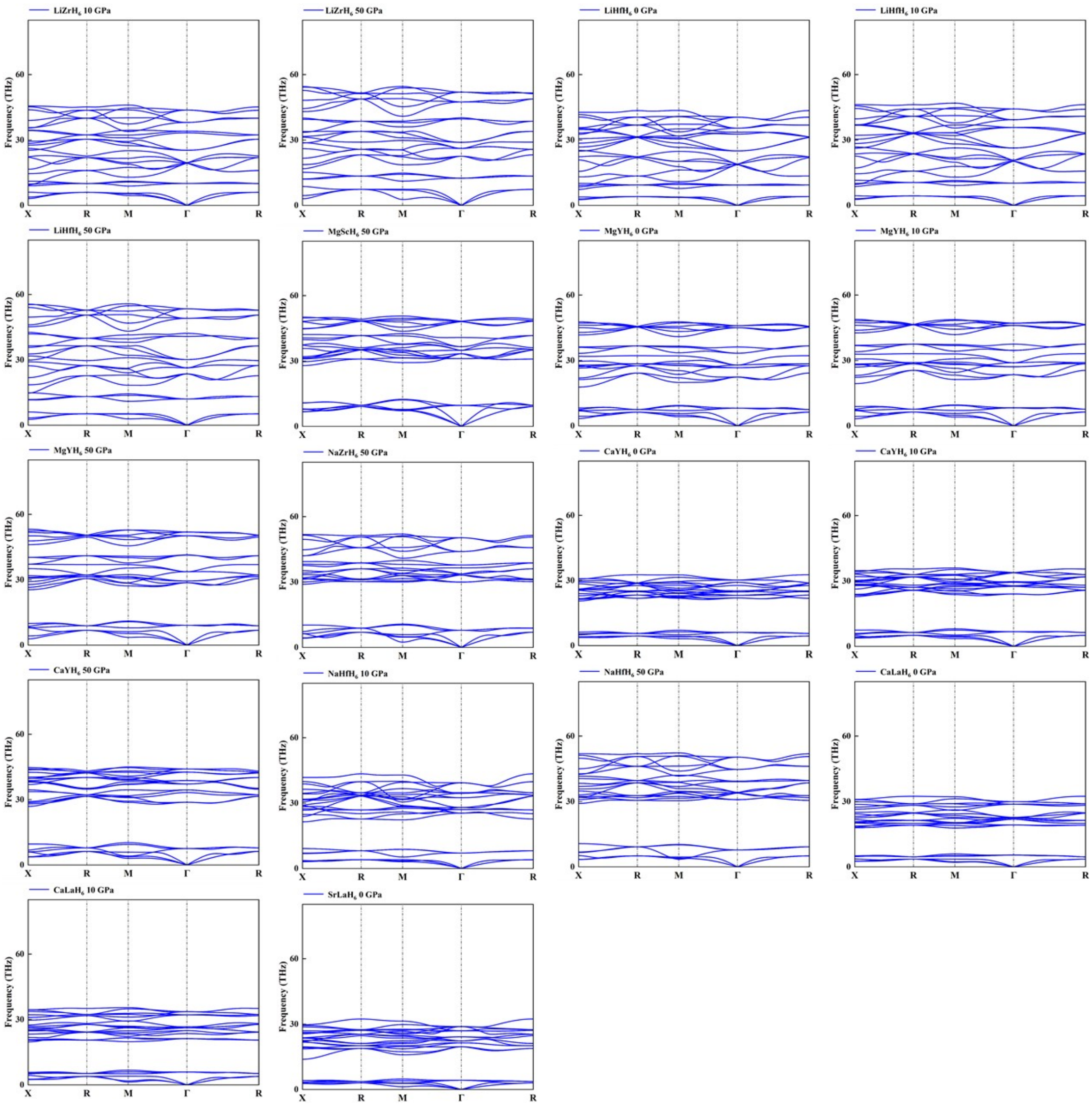

Figure S3. Calculated phonon spectrum of newly predicted ABH_6 under different pressure.

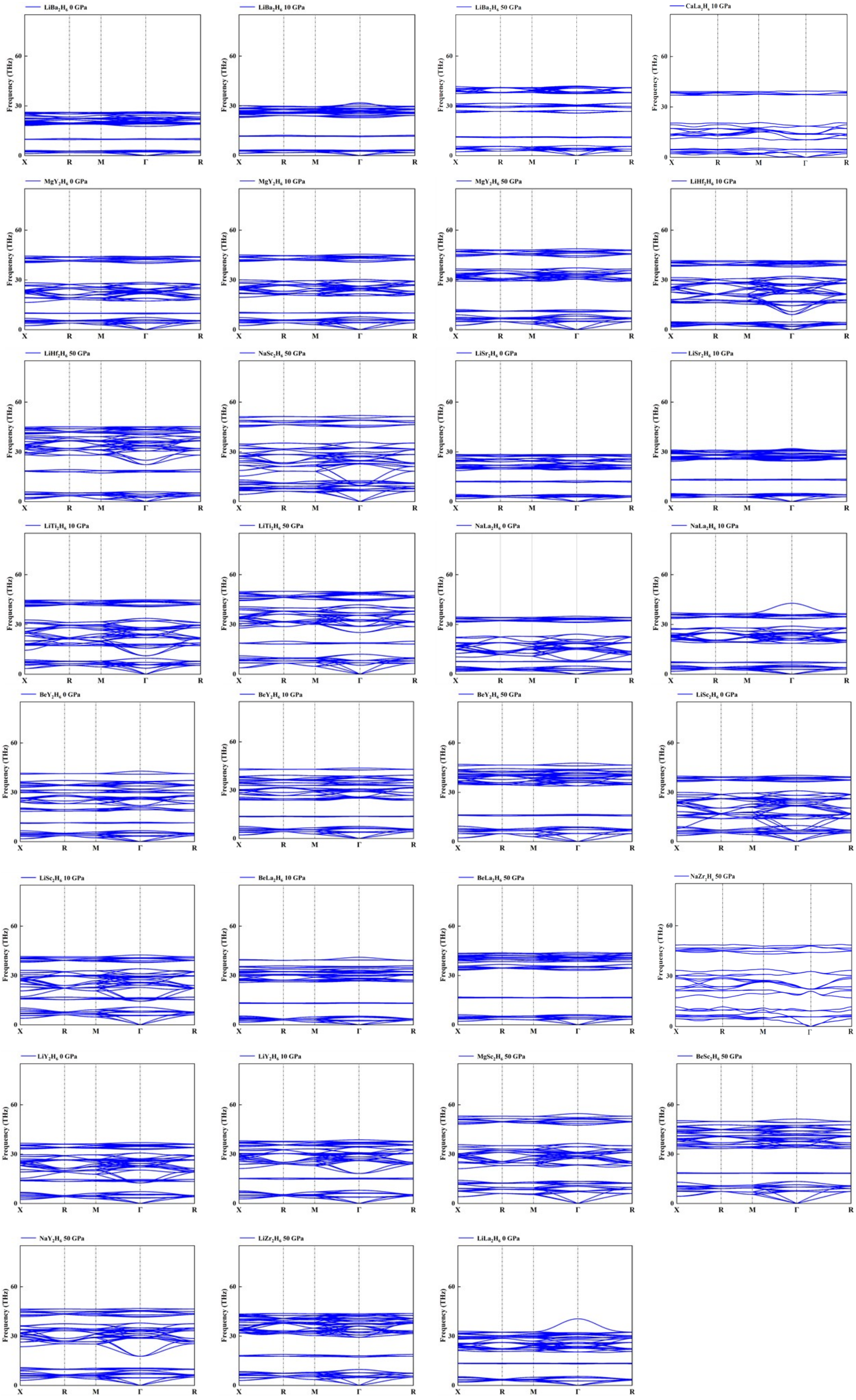

Figure S4. Calculated phonon spectrum of newly predicted AB_2H_6 under different pressure.

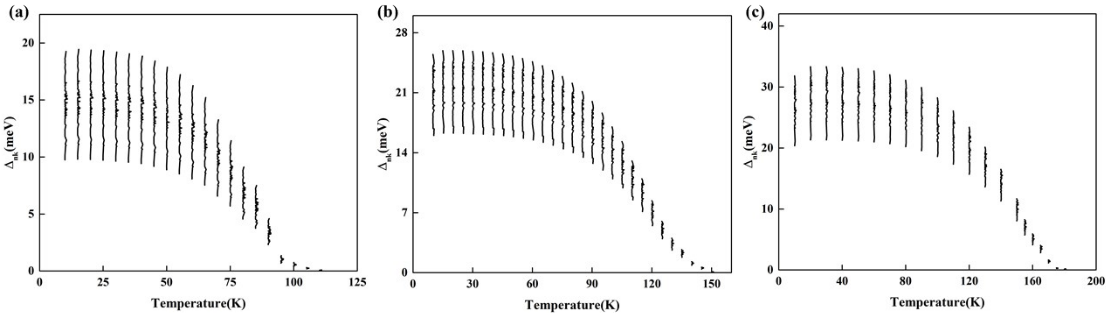

Figure S5. The superconducting energy gaps Δ_{nk} at different temperatures for $LiTiH_6$, $LiZrH_6$, and $LiHfH_6$ at 50 GPa. We have used the Wannier interpolation technique to calculate electron-phonon coupling superconductivity. The electronic and phononic states are interpolated onto fine k- and q-grids of 24x24x24, and the double Dirac δ functions for electrons and phonons are smeared out by Gaussian fucntions with widths of 50 and 0.5 meV, respectively. The Matsubara frequency is truncated at ω_c=3.0 eV, which is about twelve times the highest phonon excitation energy. The screening Coulomb potential μ* is set to be 0.1.

Table S1. Key superconducting parameters for dynamically stable ABH_3, ABH_6 and AB_2H_6 at different pressures

Phase	Pressure (GPa)	λ	ω_{log}	T_c (K)
$BeZrH_3$	50	1.9	297	41
$BeHfH_3$	50	1.8	292	39
$MgSrH_3$	0	1.8	252	34
$MgSrH_3$	10	1.3	290	30
$MgSrH_3$	50	0.7	363	14
$LiCsH_3$	50	1.0	334	26
$LiZrH_3$	50	0.9	323	21
$LiHfH_3$	50	1.0	276	20
$MgBaH_3$	0	1.5	160	19
$MgBaH_3$	10	1.5	162	19
$LiYH_3$	0	0.6	335	8
$LiYH_3$	10	0.5	389	5
$LiYH_3$	50	0.3	452	0.2
$LiLaH_3$	0	0.4	255	3
$LiLaH_3$	10	0.4	279	1
$LiLaH_3$	50	0.4	281	2
$LiScH_3$	50	0.3	627	0.4
$LiTiH_6$	50	2.3	547	87
$LiZrH_6$	10	3.0	324	58
$LiZrH_6$	50	1.7	637	82
$LiHfH_6$	0	3.5	196	37
$LiHfH_6$	10	2.8	333	58

$LiHfH_6$	50	1.6	629	80
$MgScH_6$	50	1.7	410	55
$MgYH_6$	0	2.8	173	31
$MgYH_6$	10	2.0	271	40
$MgYH_6$	50	1.4	446	49
$NaZrH_6$	50	1.2	396	37
$CaYH_6$	0	1.4	324	35
$CaYH_6$	10	1.0	426	33
$CaYH_6$	50	0.9	450	30
$NaHfH_6$	10	3.1	73	14
$NaHfH_6$	50	1.2	353	33
$CaLaH_6$	0	1.1	281	25
$CaLaH_6$	10	1.2	262	24
$SrLaH_6$	0	1.4	135	15
$MgZr_2H_6$	50	1.1	300	27
$LiBa_2H_6$	0	0.6	186	5
$LiBa_2H_6$	10	0.8	143	7
$LiBa_2H_6$	50	1.2	276	26
$CaLa_2H_6$	10	1.0	219	17
MgY_2H_6	0	0.7	365	17
MgY_2H_6	10	0.5	395	9
MgY_2H_6	50	0.3	547	0.2
$LiHf_2H_6$	10	0.8	298	14
$LiHf_2H_6$	50	0.4	387	2
$NaSc_2H_6$	50	0.5	664	13
$LiSr_2H_6$	0	0.7	339	13
$LiSr_2H_6$	10	0.7	300	11
$LiTi_2H_6$	10	0.7	347	12
$LiTi_2H_6$	50	0.3	535	1.1
$NaLa_2H_6$	0	0.6	320	9
$NaLa_2H_6$	10	0.3	502	0.5
BeY_2H_6	0	0.6	285	7
BeY_2H_6	10	0.4	356	4
BeY_2H_6	50	0.4	419	2
$LiSc_2H_6$	0	0.5	472	6
$LiSc_2H_6$	10	0.3	620	1
$BeLa_2H_6$	10	0.4	263	3
$BeLa_2H_6$	50	0.5	302	5
$NaZr_2H_6$	50	0.4	473	4
LiY_2H_6	0	0.4	446	3
LiY_2H_6	10	0.2	569	0.2
$MgSc_2H_6$	50	0.3	676	0.6
$BeSc_2H_6$	50	0.3	615	0.6

NaY_2H_6	50	0.3	754	0.6
$LiZr_2H_6$	50	0.3	458	0.5
$LiLa_2H_6$	0	0.3	355	0.2

Table S2. Possible reaction routes and formation enthalpies for $LiTiH_6$, $LiZrH_6$ and $LiHfH_6$

Material	Reaction routes	Formation enthalpy (eV)
$LiTiH_6$	$LiH+TiH+2H_2$	-0.618
$LiZrH_6$	$LiH+ZrH+2H_2$	-0.990
$LiHfH_6$	$Li+HfH_3+3/2H_2$	-1.375

Table S3. Computed superconducting parameters for $BeZrH_3$ and $MgHCu_3$.

Material	Pressure (GPa)	λ	ω_{log} (K)	T_c (K)
$BeZrH_3$	50	1.91	297.31	41.5
$MgHCu_3$	0	0.83	402.19	42.0